Physica B 406 (2011) 305–308

Contents lists available at ScienceDirect

Physica B

journal homepage: www.elsevier.com/locate/physb

Ferroelectric domain structure of the $BiFeO_3$ film grown on different substrates

H.X. Lu, J.L. Zhao, J.R. Sun *, J. Wang, B.G. Shen

Beijing National Laboratory for Condensed Matter Physics and Institute of Physics, Chinese Academy of Sciences, Beijing 100190, PR China

ARTICLE INFO

Article history:
Received 16 July 2010
Received in revised form
26 September 2010
Accepted 5 November 2010

Keywords:
Ferroelectric polarization
Domain structure
Piezoelectric force microscope

ABSTRACT

Domain structure of $BiFeO_3$ (BFO) films grown on different substrates, with a conductive $La_{0.7}Sr_{0.3}MnO_3$ underlayer, has been experimentally studied. Two oppositely orientated polarizations, along the long body diagonal to the perovskite unit cell of BFO, are detected in the BFO films on the (0 0 1)-oriented $NdGaO_3$. Electric pulses applied in the [0 0 1] direction produce a polarization switching, resulting in the domain structure characterized by the 109° domain walls. Contrary to the BFO films on $NdGaO_3$, the BFO films on $SrTiO_3$ (0 0 1) exhibit a much complex domain structure. Both 71° and 109° domain walls are possible with a uniform polarization component pointing to the bottom electrode.

© 2010 Elsevier B.V. All rights reserved.

Contents

1. Introduction

$BiFeO_3$ (BFO) has attracted great attention in recent years because of the simultaneous presence of antiferromagnetic and ferroelectric orders well above room temperature [1,2]. As has been established, the ferroelectric state of BFO is caused by a large displacement of Bi ions with respect to the FeO_6 octahedron. The polarization lies along the body diagonal to the perovskite unit cell of BFO, leading to eight polarization variants. Contrary to other ferroelectric materials, BFO exhibits a strong coupling between magnetic and electric orders, as evidenced by the electric field-induced change of spin orientation [3].

As reported, the domain structure has a strong impact on the exchange bias between BFO and the adjacent ferromagnetic layer, growing inversely with domain size [4,5]. Polarization orientation may also have an impact on exchange bias because of the strong correlation between the directions of magnetic and electric polarizations [3]. In fact, recently an enhancement of the exchange bias by 109° domain walls has been detected [5]. There are also signatures that the polarization switching under electric field may depend on domain structure [6]. It is therefore clear that it would be useful to get a feasible control of domain structure of BFO.

It has been found that the domain structure of BFO is sensitive to crystal orientation. Three kinds of domain walls, namely 71°, 109°, and 180° domain walls, exist in the BFO film grown on the (0 0 1)-orientated $SrTiO_3$ (STO). However, the strip-featured domains are formed in the films grown on 0.8°-miscut STO and $DyScO_3$ (1 1 0) substrates [4]. Most of these works concentrated on the BFO films grown on STO and $DyScO_3$ with $SrRuO_3$ as a bottom electrode [1,4,7]. Different from the cubic STO, $NdGaO_3$ (NGO) is orthorhombic with the lattice constants of $a=5.429$ Å, $b=5.498$ Å, and $c=7.710$ Å. The deduced lattice parameters for the deformed perovskite unit cell are $a_0=b_0=3.863$ Å and $c_0=3.855$ Å, and $\gamma \approx 90.7°$ (γ is the angle between a_0 and b_0 axes). The different symmetry of NGO from STO and a large lattice mismatch between NGO and BFO (~3.4%) may assign the domain structure some new features. Based on this consideration, in this letter we performed a systematic study on the domain structure of the BFO film grown on NGO (0 0 1). As experimentally revealed, the domain structure of BFO/$La_{0.7}Sr_{0.3}MnO_3$/NGO is rather simple, formed only by two oppositely directed polarizations. Electric pulses can produce

* Corresponding author. Tel.: +86 10 82648075; fax: +86 10 82649485.
E-mail address: jrsun@g203.iphy.ac.cn (J.R. Sun).

0921-4526/$ - see front matter © 2010 Elsevier B.V. All rights reserved.
doi:10.1016/j.physb.2010.11.011

polarization rotation, resulting in a transition of the domain walls from 180° to 109°. In contrast, the BFO films on STO (0 0 1) exhibit a much complex domain structure characterized by 71° and 109° domain walls.

2. Experiments

The sample was prepared by the pulsed laser ablation technique. As bottom electrode, a $La_{0.7}Sr_{0.3}MnO_3$ (LSMO) layer of 80 nm was first grown on NGO (0 0 1) at the substrate temperature of ~700 °C and the oxygen pressure of ~46 Pa. A BFO layer of 50 nm was then deposited at a lower temperature, ~630 °C, and a lower oxygen pressure, ~15 Pa. The film was subsequently furnace-cooled to room temperature in an oxygen atmosphere of ~200 Pa. For a comparison study, BFO films on the STO (0 0 1) substrates were also prepared following the same procedure.

The structure of the films was analyzed by an X-ray diffractometer with the Cu Kα radiation (Philips X'pert Pro diffractometer). The surface morphology and domain structure of the BFO film were analyzed by a piezoelectric force microscope (PFM) (Nanonavi E-Sweep). During PFM measurements, an ac bias with the frequency of 6 kHz and amplitude of 6 V, for the Au tip, or 14–16 V, for the Rh tip, was applied between the tip and the LSMO electrode. In our equipment, the amplitude of the piezoelectric response was recorded, translated into electric signals, in the unit of mV. All the measurements were performed at room temperature.

3. Results and discussions

Fig. 1 shows the X-ray diffraction (XRD) pattern with clean BFO and LSMO peaks, without impurity phases for the 2θ angle from 15° to 80°. The deduced out-of-plane lattice constants are 4.182 and 3.854 Å for the films on NGO and 4.077 and 3.852 Å for the films on STO. The latter two lattice parameters are consistent with the reported values of ~4.051 and ~3.860 Å for the corresponding films on STO [1,8].

As revealed by the atomic force microscope analysis, the film is rather smooth. For the BFO/LSMO/NGO film, the root-mean-square roughness is ~4 Å, and the general peak-to-valley fluctuation is ~15 Å. Fig. 2 shows the PFM image of BFO, measured with the long cantilever lining along the directions marked in the figure. Island-shaped dark areas, like rilievos on bright background, are observed in the out-of-plane (OP) images, independent of the scanning direction (Fig. 2(a) and (b)). Sometimes these islands link together, forming a network-featured domain structure (Fig. 2(b)). From a first glance, the populations of bright and dark domains are different, and a rough estimation gives an up-to-down domain ratio of 60–70% (see the context). It indicates the presence of a

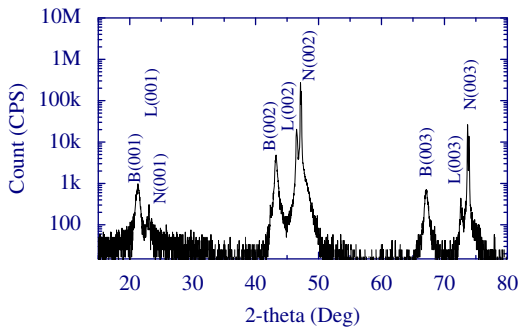

Fig. 1. XRD patterns of BFO/LSMO/NGO film, measured at ambient temperature. The labels B, L, and N in the figure represent BFO, LSMO, and NGO, respectively. The indices are based on the simple perovskite unit cell.

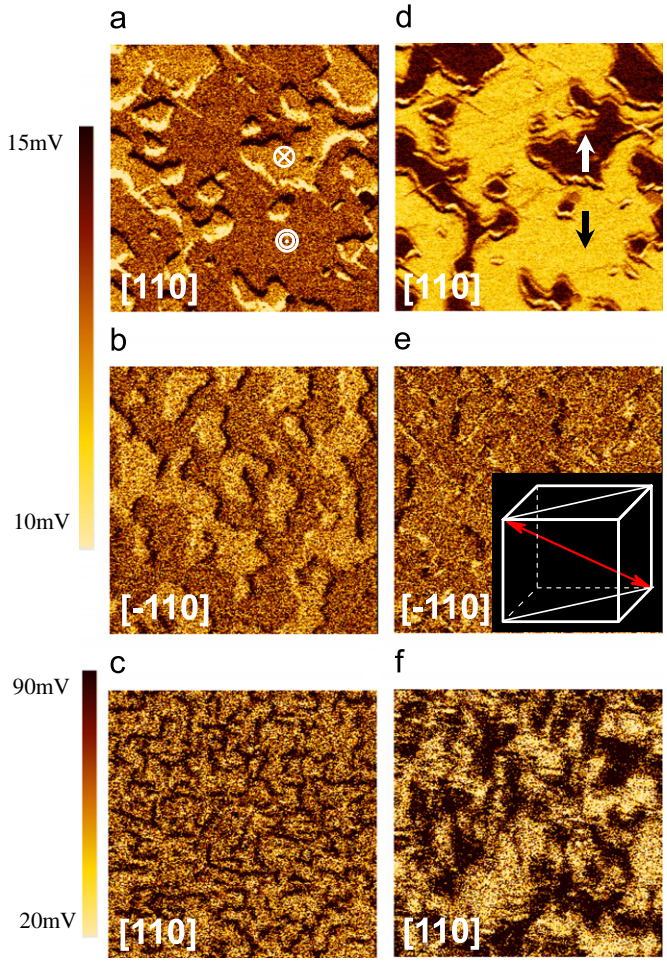

Fig. 2. Domain structure of BFO/LSMO/NGO, measured with the cantilever pointing along the directions marked in the figure. (a), (b), and (c) are OP–PFM images, and (d), (e), and (f) are the corresponding IP–PFM images. The scale of the image is $2 \times 2\ \mu m^2$ for (a), (c), (d), and (f) and $2.5 \times 2.5\ \mu m^2$ for (b) and (e). Inset plot in (e) is a sketch of possible polarization configuration. Symbols and arrows in the figure mark the direction of OP and IP components of the polarization, respectively.

preferred orientation for the polarization in this film. As well established, the upward polarization will give rise to a dark image, while the downward one yields a bright contrast. The two color tones thus imply two OP components of the polarizations in the [0 0 1] and [0 0 $\bar{1}$]directions, respectively. In contrast, no obvious color contrast, except for the slightly dark labyrinth-like domain walls, is observed in the PFM image of BFO/LSMO/STO (Fig. 2(c)).

Based on the data in Fig. 2(a) and (b), three kinds of domain walls are possible in BFO/LSMO/NGO, namely the 180°-angled polarizations and the 71° or 109°-angled polarizations that have opposite OP projections. Unlike BFO/LSMO/NGO, the domains in BFO/LSMO/STO may have the same downward component. As experimentally revealed, a downward electric field causes an upward polarization switching (not shown). In this case, only two possible domain walls 71° and 109° are possible. The BFO/LSMO/STO films are also different from the thick BFO/$SrRuO_3$/STO films, for which mosaic-shaped domain structures with both upward and downward OP components are observed [7].

For a further investigation on polarization orientation, the in-plane (IP) piezoelectric responses are studied. Different from the OP image, the color contrast in the IP images of BFO/LSMO/NGO depends strongly on the set up of the cantilever. The domain structure is unclear when the cantilever lines along the [$\bar{1}$ 1 0]direction, and sometimes only humilis marks corresponding

to the OP domains can be identified (Fig. 2(e)). However, an image with an evident dark-bright contrast emerges after rotating the sample by 90° (Fig. 2(d)). This phenomenon is observed in images from different locations of the film. A further observation is the exact correspondence of the domain patterns even the details in the IP and OP images (Fig. 2(a) and (d)).

As has been established, the piezoelectric response is maximum/minimum when the IP component is perpendicular/parallel to the long cantilever. The systematic variation of the IP image as film rotates therefore suggests a preferred orientation of the IP component along the $[\bar{1}\,1\,0]$direction. This kind of IP image can be produced either by two oppositely directed polarizations or by two polarizations that form an angle of 109° but have the same OP component. Considering the fact that the polarizations with similar OP projection cannot show the domain structure in the OP image, the polarizations in BFO/LSMO/NGO must be 180°-angled. Contrary to BFO/LSMO/NGO, the IP images of the BFO/LSMO/STO films show obvious color contrast, regardless of the set up of the cantilever (Fig. 2(f)). The polarizations in this film may form the angles of both 71° and 109° but have a downward directed OP component.

As revealed in the XRD analysis, $[\bar{1}\,1\,1]$ is the long diagonal of the pseudocubic unit cell of NGO. It should be noted that the IP component of polarization aligns exactly in the $[\bar{1}\,1\,0]$ direction. This suggests a close relation between lattice strains and polarizations. The BFO film prefers to polarize in the less strained long body diagonal to the unit cell of BFO, as schematically shown in the inset plot of Fig. 2(e) (only the polarization orientation along one of the two long diagonals is shown here).

Further evidence for the structural–ferroelectric correlation is also obtained. As shown in Fig. 3, grain boundaries are generally the domain boundaries (marked by black arrows). However, the opposite is not true; two or more ferroelectric domains can occur within one crystal grain. A remarkable observation is that the domains' boundary in the grains is usually delimited by a raised and narrow edge (marked by white arrows). It could be a distinctive structure feature due to the piezoelectric effect of two differently orientated domains. Coinciding with the narrow edge, there is a transition region, ~500 Å in width, between two domains (Fig. 2(a) and (d)). It has a color tone even much brighter than that of the domains below. Similarly, the domain walls located at the grain boundaries show a much darker color than that of the domains above. It seems that the domain borders are much more susceptible to the electric field than the domain itself. A complex decoration of the domain border is also observed in the IP images (Fig. 2(d)). As well known, the BFO film is compressively strained. However, lattice strains at the grain boundaries and ridges within the grains could be partially relaxed, which may be the origin of the enhanced piezoelectric response.

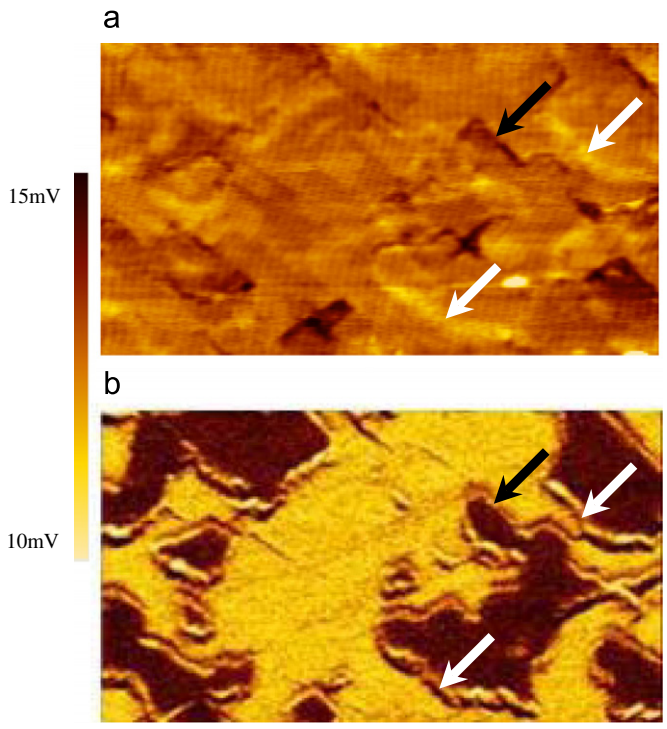

Fig. 3. Surface morphology (a) and the corresponding IP–PFM image (b) of BFO/LSMO/NGO. The white and black arrows in (a) mark, respectively, the raised strip and grain boundaries that correspond to the domain boundaries in (b). The scale of the image size is $2 \times 1\ \mu m^2$.

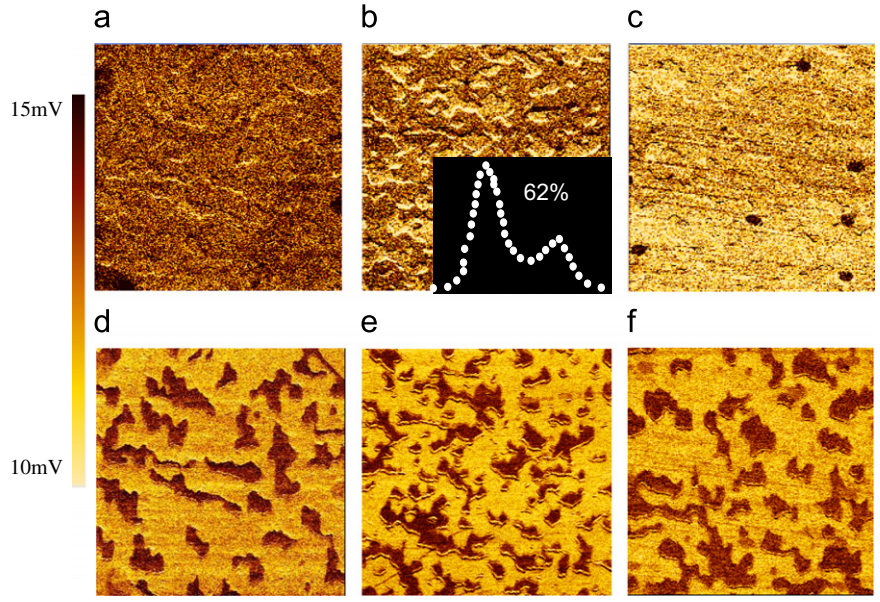

Fig. 4. Domain structure of BFO/LSMO/NGO processed under electric pulses, measured with the cantilever pointing along the [1 1 0] direction. (a), (b), and (c) are OP–PFM images, and (d), (e), and (f) are the corresponding IP–PFM images. The applied pulses are −30, 0 and 30 V for (a), (b), and (c), respectively. The image size is $5 \times 5\ \mu m^2$. Inset plot in (b) shows the population of the color tone in (e). Based on the areas below the two peaks; population of the two domains (~62%) is calculated.

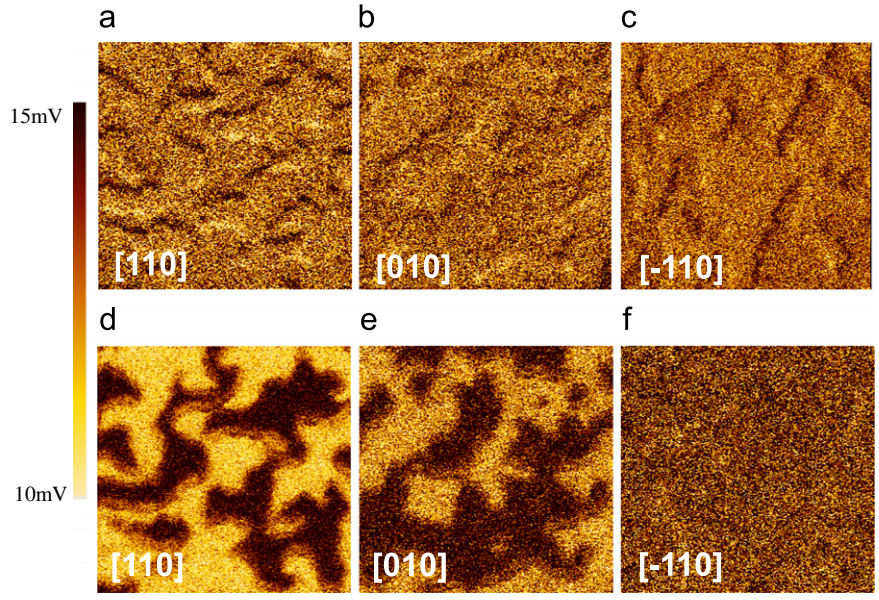

Fig. 5. PFM images of the film area near the negative electrode, measured with the cantilever pointing along the directions marked in the figures. (a), (b), and (c) are OP–PFM images, and (d), (e), and (f) are the corresponding IP–PFM images. The scale of the PFM image is $2 \times 2\ \mu m^2$.

For a study of the dynamitic switching of ferroelectric domains, PFM images of the BFO/LSMO/NGO films were further measured after a processing of electric pulses. Two In electrodes of the size $\sim 2 \times 2\ mm^2$ were pasted to the film surface. Biases directing from In to LSMO are defined as positive ones. Short positive pulses, with the amplitude of 30 V and the width of 10 ms, were applied to the BFO film through one of the two In electrodes and the below LSMO electrode, while the negative pulses were applied through another In-LSMO pair. PFM images of the film planes covered by the In electrodes were measured. As shown in Fig. 4(a) and (b), the original downward domains become dark under negative pulses while the upward domains are essentially unaffected. As a consequence, differences between the domains are unclear for the OP image. This result indicates the field-induced down-to-up polarization switching. In contrast, the overall color of the OP image becomes bright when the film is treated by positive pulses, due to the darkening of the original downward domains (Fig. 4(c)).

Contrary to the OP images, the IP ones show a sharp color contrast (Fig. 4(d–f)), which indicates the presence of different ferroelectric domains after pulse processing. These results indicate that the change in the OP component under electric pulses does not eliminate the contrast in the IP image. We also measured the PFM image by rotating the sample in different angles after electric pulse treatments (-30 V). As shown in Fig. 5, the color contrast first weakens then completely vanishes after rotating the film by 45° and 90°, whereas the OP component remains essentially unchanged. Based on the above analyses, only 109° polarizations can yield the same OP component but different IP projections. This implies that the transition of the domain walls from 180° to 109° caused electric pulses, though the polarizations remain in the (1 1 0) plane. As recently reported, this kind of domain structure may favor an enhanced exchange bias between BFO and the adjacent magnetic layer [5].

4. Summary

In summary, the domain structure of the BFO films grown on different substrates has been experimentally studied. Two oppositely orientated polarizations, along the long body diagonal to the pseudocubic unit cell of BFO, are observed in the BFO films on NGO (0 0 1). Electric pulses applied in the [0 0 1] produce a polarization switching, resulting in the domain structure characterized by the 109° domain walls. Contrary to the BFO films on NGO, the BFO films on STO (0 0 1) exhibit a much complex domain structure, and both 71° and 109° domain walls are possible, with a uniform polarization component pointing to the bottom electrode.

Acknowledgements

This work has been supported by the National Natural Science Foundation of China, the National Fundamental Research of China, and the Knowledge Innovation Project of the Chinese Academy of Sciences.

References

[1] J. Wang, J.B. Neaton, H. Zheng, V. Nagarajan, S.B. Ogale, B. Liu, D. Viehland, V. Vaithyanathan, D.G. Schlom, U.V. Waghmare, N.A. Spaldin, K.M. Rabe, M. Wuttig, R. Ramesh, Science 299 (1719) 2003.
[2] Ho Won Jang, Daniel Ortiz, Seung-Hyub Baek, Chad M. Folkman, Rasmi R. Das, Padraic Shafer, Yanbin Chen, Christofer T. Nelson, Xiaoqing Pan, Ramamoorthy Ramesh, Chang-Beom Eom, Adv. Mater. 21 (2009) 817.
[3] Ying-hao Chu, Lane W. Martin, Mikel B. Holcomb, Martin Gajek, Shu-jen Han, Qing He, Nina Balke, Chan-ho Yang, Donkoun Lee, Wei Hu, Qian Zhan, Pei-ling Yang, Arantxa Fraile-rodríguez, Andreas Scholl, Shan X. Wang, R. Ramesh, Nat. Mater. 7 (2008) 478.
[4] H. Béa, M. Bibes, F. Ott, B. Dupé, X.-H. Zhu, S. Petit, S. Fusil, C. Deranlot, K. Bouzehouane, A. Barthélémy, Phys. Rev. Lett. 100 (2008) 017204.
[5] Lane W. Martin, Ying-Hao Chu, Mikel B. Holcomb, Mark Huijben, Pu Yu, Shu-Jen Han, Donkoun Lee, Shan X. Wang, R. Ramesh, Nano Lett. 8 (2008) 2050.
[6] F. Zavaliche, S.Y. Yang, T. Zhao, Y.H. Chu, M.P. Cruz, C.B. Eom, R. Ramesh, Phase Transit. 79 (2006) 991.
[7] M.P. Cruz, Y.H. Chu, J.X. Zhang, P.L. Yang, F. Zavaliche, Q. He, P. Shafer, L.Q. Chen, R. Ramesh, Phys. Rev. Lett. 99 (2007) 217601.
[8] P. Orgiani, A. Yu., C. Petrov, C. Adamo, C. Aruta, G.M. Barone, A. De Luca, M. Galdi, D. Polichetti, Zola, L. Maritato, Phys. Rev. B 74 (2006) 134419.